A&A 376, L27–L30 (2001)
DOI: 10.1051/0004-6361:20010990

Astronomy & Astrophysics

Letter to the Editor

Discovery of depressions in the X-ray emission of the distant galaxy cluster RBS797 in a CHANDRA observation

S. Schindler[1], A. Castillo-Morales[1], E. De Filippis[1], A. Schwope[2], and J. Wambsganss[3]

[1] Astrophysics Research Institute, Liverpool John Moores University, Twelve Quays House, Birkenhead CH41 1LD, UK
[2] Astrophysikalisches Institut Potsdam, An der Sternwarte 16, 14482 Potsdam, Germany
[3] Universität Potsdam, Institut für Physik, Am Neuen Palais 10, 14469 Potsdam, Germany

Received 14 May 2001 / Accepted 9 July 2001

Abstract. We present CHANDRA observations of the X-ray luminous, distant galaxy cluster RBS797 at $z = 0.35$. In the central region the X-ray emission shows two pronounced X-ray minima, which are located opposite to each other with respect to the cluster centre. These depressions suggest an interaction between the central radio galaxy and the intra-cluster medium, which would be the first detection in such a distant cluster. The minima are symmetric relative to the cluster centre and very deep compared to similar features found in a few other nearby clusters. A spectral and morphological analysis of the overall cluster emission shows that RBS797 is a hot cluster ($T = 7.7^{+1.2}_{-1.0}$ keV) with a total mass of $M_{\rm tot}(r_{500}) = 6.5^{+1.6}_{-1.2} \times 10^{14} M_{\odot}$.

Key words. galaxies: clusters: general – intergalactic medium – cosmology: observations – cosmology: theory – dark matter – X-rays: galaxies

1. Introduction

Interaction between the intra-cluster gas and radio sources in the centre of galaxy clusters has been found in several nearby clusters with an anticorrelation of X-ray emission and radio emission, e.g. in the Perseus cluster (Fabian et al. 2000), in Hydra-A (McNamara et al. 2000), and in Abell clusters A4059 (Huang & Sarazin 1998), A2597 (McNamara 2001), A2052 (Sarazin 2001), A2199 (Fabian 2001), and A2634 (Schindler 1996). Such an interaction of two different components is particularly interesting because one can infer physical conditions and processes in the cluster centre, e.g. heating and cooling effects, magnetic fields or energies of relativistic particles, from the pressure balance. The observations suggest that the cavities in the X-ray gas rise outwards by buoyancy (McNamara et al. 2000; Churazov et al. 2000) while a model by Heinz et al. (1998) predicts shocked gas around the cavities which is not observed. Models by Reynolds et al. (2001) and David et al. (2000) suggest a weak shock regime with radio lobes moving at the local sound speed.

We present here recent CHANDRA observations of the galaxy cluster RBS797. They reveal clear X-ray minima in the cluster centre. We hypothesise that these minima are caused by interaction between the radio source embedded in the central cluster galaxy and the intra-cluster medium. RBS797 would be the first *distant* cluster in which evidence for such interaction has been found. Only the high spatial resolution of CHANDRA makes it possible to observe such details in distant clusters. This X-ray observation is part of a broader programme to search for strong gravitational lensing in X-ray selected, X-ray luminous clusters. The goal is to take both deep optical images of these clusters and high resolution X-ray exposures. In this way we can use the clusters for arc statistics as well as for the determination and comparison of cluster masses estimated by X-ray observations and by gravitational lensing. Throughout this paper we use $H_0 = 50$ km/s/Mpc and $q_0 = 0.5$.

2. Cluster identification

The X-ray source RXS J094713.2+762317 (or RBS797), found in the ROSAT All-Sky Survey (RASS), was observed optically in the course of the ROSAT Bright Survey (RBS), aiming at optical identification of all bright (count rate $> 0.2\,{\rm cts\,s^{-1}}$), high-galactic latitude ($|b| > 30°$) X-ray sources detected in the RASS (Fischer et al. 1998; Schwope et al. 2000). A spectrum of the central cluster galaxy at RA(2000) = 09 47 12.5, DEC(2000) = +76 23 14, taken with the SAO 6 m telescope shows a strong O[II]λ3727 emission line, and weak, narrow Hβ

Send offprint requests to: S. Schindler,
e-mail: sas@astro.livjm.ac.uk

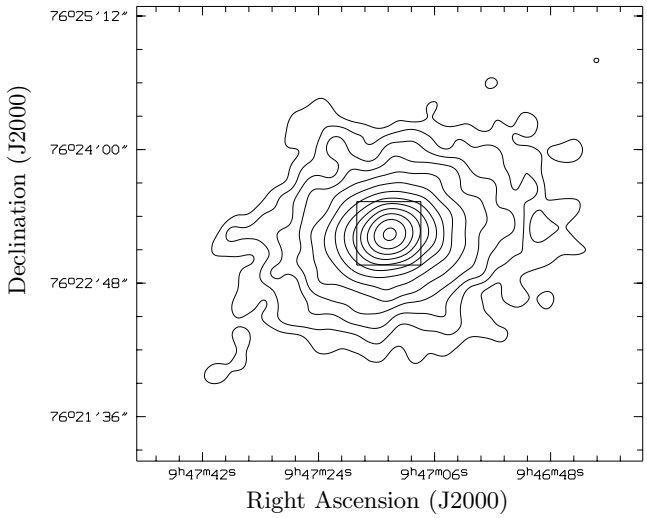

Fig. 1. CHANDRA image of the cluster RBS797. The cluster is relatively regular with an ellipticity of 1.3–1.4 in E-W direction. The contours are logarithmically spaced with 5 contours per decade and the highest corresponding to 3.9 cts/s/arcmin^2. The image is smoothed with a Gaussian of $\sigma = 5$ arcsec. The size of the image is 4.7 arcmin on the side. The central square marks the region shown with higher resolution in Fig. 2.

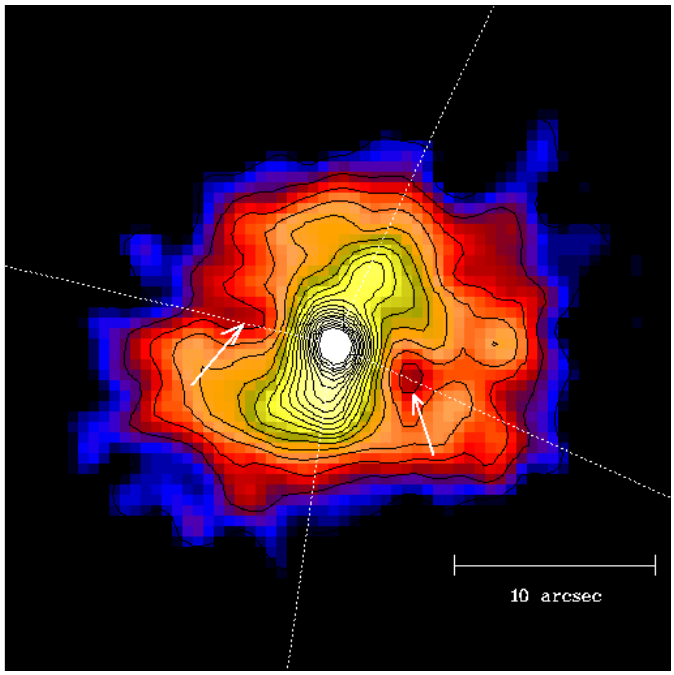

Fig. 2. X-ray image of the central (32 arcsec)^2 of the cluster RBS797. There are clear minima in the X-ray emission in ENE and WSW direction at about 5 arcsec from the cluster centre (see arrows). An excess of emission is found in perpendicular directions. The dotted lines mark the traces shown in Fig. 3. The contours have a linear spacing of 0.7 cts/s/arcmin^2 with the highest being 14 cts/s/arcmin^2. The image is smoothed with a Gaussian of $\sigma = 0.75$ arcsec.

and O[III]$\lambda\lambda$4959/5007 emission lines at a redshift of $z = 0.354$. The emission lines can be due to a cooling flow or due to nuclear activity of the central cluster galaxy.

3. X-ray observation of RBS797 with CHANDRA

RBS797 was observed on October 20th, 2000 with the CHANDRA Advanced CCD Imaging Spectrometer (ACIS) I detector for a total exposure time of 13.3 ks. No time was lost due to flares. For the data analysis we used the standard set of event grades and applied no a priori filtering. The energy range used for the images is 0.5–7 keV, for the spectra it is given in Table 1. The response matrices from the CHANDRA Calibration Database package (CALDB) version 2.0 are used.

Figure 1 shows the X-ray image of the cluster RBS797 on a scale of 4.7 arcmin ($\equiv$1.7 Mpc). The cluster emission is elliptical with axis ratios of major to minor axis varying slightly from 1.3 at a radius of 0.26 arcmin to 1.4 at a radius of 1.7 arcmin. The centre and the position angle ($\approx -70°$, N over E) of the ellipses are almost the same over the entire radius range.

The innermost (32 arcsec)^2 region of the galaxy cluster RBS797 is shown in Fig. 2. Two emission minima are obvious in ENE and WSW direction at distances of about 3–5 arcsec from the cluster centre. The minima are opposite to each other with respect to the cluster centre. In perpendicular directions excess X-ray emission is visible. At radii of 4 arcsec there is a factor of 3–4 between the X-ray emissions from the different regions (see Fig. 3). The sizes of the X-ray depressions are about 20–30 kpc. It is likely – but largely a hypothesis up to now – that the gas has been pushed from the low X-ray emission regions to the high X-ray emission regions by the pressure of relativistic particles in radio lobes, as has been observed in a number of nearby clusters. Although a good hardness ratio map cannot be derived from the data due to the limited number of photons, we find that the hardness ratio in the depressions is not harder than than the overall cluster emission, which excludes absorption or hot gas bubbles as explanations for the minima. The depressions are very significant and deep, and also very symmetric compared to other clusters. Therefore this cluster appears to be an ideal object to investigate the interaction of jets and the intra-cluster medium. We will study the interaction in detail with radio follow-up observations.

4. Spectral analysis, luminosity and mass determination

The CHANDRA data can be used to derive the temperature, metallicity, luminosity and mass of RBS797. For the spectral fits the energy range is restricted to 0.5–10 keV and 2–10 keV, respectively, because the calibration of the low energy channels is still uncertain. We treat the central point-like source (radius $\lesssim$2 arcsec) separately, because this source is probably an AGN, which would distort the thermal spectrum of the intra-cluster gas.

The results of the spectral analysis are summarised in Table 1. The overall emission is well fit by a thermal bremsstrahlung model with a temperature of 7.7 keV and

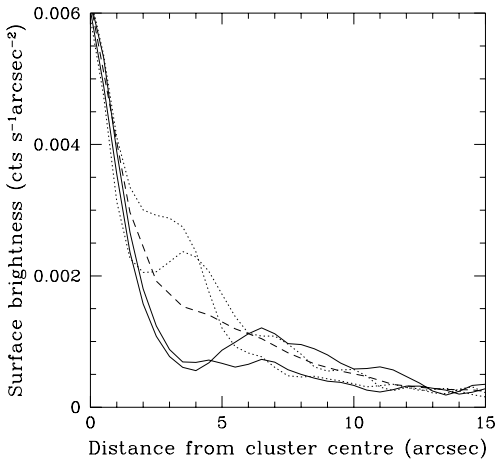

Fig. 3. Dependence of the surface brightness on direction: the X-ray emission from the centre in direction of the minima (solid lines, position angles 77° and 243°, N over E) and in direction of the maxima (dotted lines, position angles 171° and 337°). There is an X-ray deficit of a factor of 3–4 in the "holes" compared to the perpendicular directions. The dashed line shows an average profile integrated over all angles. A surface brightness of 0.001 cts/s/arcsec^2 corresponds to 3 counts per ACIS pixel (0.5 arcsec on the side).

a metallicity around 0.26 in solar units when the hydrogen column density is fixed to the Galactic value (Dickey & Lockman 1990). We find somewhat higher temperatures for fits in the 0.5–10 keV band, compared to the results of the 2–10 keV band, probably indicating problems with the calibration of the low energy channels. Attempting to see radial variations in the fit parameters, we extract photons from three different annuli. There is a trend of increasing temperature and decreasing metallicity with radius, which, however, is not statistically significant due to the limited number of photons in this pointing.

The best-fit value for the redshift ($z = 0.39 \pm 0.02$) is slightly higher than the optically determined redshift ($z_{\rm opt} = 0.354$), but they still agree with each other within 2σ. If we fix the redshift to the optical value, the resulting metallicity is lower because the location of the Fe lines does not correspond well with the bump in the observed X-ray spectrum.

Although the "arms" – the regions of higher emission surrounding the minima – contain only 1387 source counts, we attempt a spectral fit, because the temperature measurement is important for distinguishing different models. We find a slightly lower temperature (4.4 keV, see Table 1) than for the rest of the cluster, suggesting that the "arms" are probably not shocked regions. This would rule out the model by Heinz et al. (1998). Similar results have been found in other clusters (Fabian et al. 2000; McNamara et al. 2000).

In the centre of the cluster is a point-like source, which has a source count rate of about 0.026 cts/s and a flux $F_{\rm centre}(2\text{–}10\ {\rm keV}) = 2.2 \times 10^{-13}$ erg/s/cm^2. The spectrum of this source is very flat and cannot be fitted with a thermal spectrum of reasonable temperature. A power law spectrum, which is an indication for an AGN, (and also a sum of a power law and a thermal spectrum) yields a good fit with a very low index of 1.2 ± 0.2.

The NRAO VLA Sky Survey (NVSS) lists a radio source at the central cluster position with a peak flux of 0.02 Jy/beam (Condon et al. 1998) which is another indication for an active galaxy in the centre of the cluster. A complementary explanation for the central X-ray peak would be a cooling flow as the central cooling time is $\approx 10^9$ yr.

The X-ray emission of the cluster can be traced out to a radius of 4.1 arcmin ($\equiv$1.5 Mpc). Within this radius there are 11 000 source counts. For the above mentioned parameters, this corresponds to a flux of $f_{\rm X}(0.5\text{–}7.0\ {\rm keV}) = 7.1 \times 10^{-12}$ erg/s/cm^2 and $f_{\rm X}({\rm bol}) = 1.1 \times 10^{-11}$ erg/s/cm^2 and for a redshift of $z = 0.354$ to a luminosity of $L_{\rm X}(0.5\text{–}7.0\ {\rm keV}) = 4.0 \times 10^{45}$ erg/s and $L_{\rm X}({\rm bol}) = 6.7 \times 10^{45}$ erg/s. Only 3% of the total emission comes from the central source.

The X-ray surface brightness profile of RBS797 (centred on the central galaxy) can be fitted well by a β model (Cavaliere & Fusco-Femiano 1976) when ignoring the central region. A fit excluding the central 6 arcsec radius yields a slope $\beta = 0.63 \pm 0.01$, a core radius $r_{\rm c} = 8.1(\pm 0.6)$ arcsec [or 49($\pm$4) kpc] and a central surface brightness $S_0 = 6.6$ cts/s/arcmin^2. With the assumption of spherical symmetry this corresponds to a gas mass of $M_{\rm gas}(1\ {\rm Mpc}) = 0.90(\pm 0.07) \times 10^{14}\ M_\odot$ and $M_{\rm gas}(r_{500}) = 1.13(\pm 0.09) \times 10^{14}\ M_\odot$ with $r_{500} = 1.22(\pm 0.08)$ Mpc. Assuming hydrostatic equilibrium, the total mass of the cluster can be estimated. For an isothermal cluster of $T = 7.7$ keV the total mass is $M_{\rm tot}(1\ {\rm Mpc}) = 5.3^{+0.8}_{-0.7} \times 10^{14}\ M_\odot$ and $M_{\rm tot}(r_{500}) = 6.5^{+1.6}_{-1.2} \times 10^{14}\ M_\odot$ (see Fig. 4). This corresponds to a gas mass fraction $f_{\rm gas}(r_{500}) = 0.17^{+0.06}_{-0.05}$ which is in good agreement with the gas mass fractions found in samples of nearby and distant clusters (Ettori & Fabian 1999; Mohr et al. 1999; Schindler 1999). Taking into account the temperature gradient changes the results slightly (see Fig. 4).

5. Summary

The X-ray luminous cluster RBS797 reveals remarkable depressions in the X-ray emission of the central region. The depressions are roughly circular and arranged symmetrically with respect to the cluster centre. They have diameters of 20–30 kpc and are very deep: a factor of 3–4 less emission than in the other directions. The discovery of these minima shows the ability of CHANDRA to investigate physical effects even in clusters as distant as RBS797 ($z = 0.35$).

The spectral and morphological analysis of RBS797 shows that the cluster has a high temperature of $T = 7.7$ keV, a metallicity $Z = 0.2\text{–}0.3$, and a high luminosity $L_{\rm X}({\rm bol}) = 6.7 \times 10^{45}$ erg/s. The total mass within r_{500} is $M_{\rm tot}(r_{500}) = 6.5 \times 10^{14}\ M_\odot$ with a gas mass fraction $f_{\rm gas}(r_{500}) = 0.17$. In follow-up radio observations the

Table 1. Results of the spectral fits to the X-ray emission of the galaxy cluster RBS797. Column 1 shows the radii in arcsec of the region, from which the photons have been extracted. Column 2 lists the model used for the fit: MeKaL = Kaastra & Mewe (1993), Liedahl et al. (1995), PL = power law. Column 3 lists the energy range. In Cols. 4-7 the fit parameters are given: hydrogen column density in 10^{20} cm^{-2}, temperature in keV (for power law fits it is the power law index), metallicity in solar units, redshift. The errors are 90% confidence levels. Columns 8 and 9 are the degrees of freedom of the fit and the reduced χ^2.

1	2	3	4	5	6	7	8	9
radius in arcsec	model	energy range in keV	$n_{\rm H}$ in 10^{20} cm^{-2}	temp. kT in keV	metallicity Z in solar units	redshift z	d.o.f.	χ^2/d.o.f.
2−80	MeKaL	0.5−10	2.22(fixed)	$7.7^{+1.2}_{-1.0}$	0.26 ± 0.10	0.39 ± 0.02	272	1.2
2−80	MeKaL	0.5−10	$6.1^{+1.5}_{-1.4}$	6.3 ± 0.6	0.26 ± 0.09	0.38 ± 0.02	271	1.1
2−80	MeKaL	2−10	2.22(fixed)	$8.1^{+1.6}_{-1.5}$	0.25 ± 0.12	0.39 ± 0.02	109	0.9
2−80	MeKaL	2−10	2.22(fixed)	$7.4^{+1.7}_{-1.1}$	0.17 ± 0.11	0.354(fixed)	91	1.0
2−10	MeKaL	0.5−10	2.22(fixed)	$5.7^{+0.7}_{-0.5}$	$0.38^{+0.17}_{-0.16}$	0.39(fixed)	117	1.6
10−30	MeKaL	0.5−10	2.22(fixed)	$8.4^{+1.2}_{-1.0}$	0.25 ± 0.18	0.39(fixed)	139	1.0
30−80	MeKaL	0.5−10	2.22(fixed)	$11.7^{+4.3}_{-2.5}$	$0.20^{+0.35}_{-0.20}$	0.39(fixed)	95	1.2
arms	MeKaL	0.5−10	2.22(fixed)	$4.4^{+0.7}_{-0.6}$	0.26(fixed)	0.39(fixed)	52	1.2
0−2	PL	0.5−10	2.22(fixed)	1.2 ± 0.2	-	0.39(fixed)	20	0.9
0−2	0.59×MeKal + 0.41×PL	0.5−10	2.22(fixed)	7.7(fixed) 1.1 ± 0.2	0.26(fixed)	0.39(fixed)	19	0.9

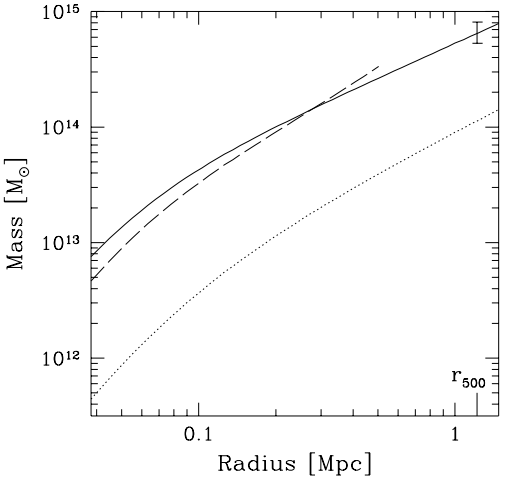

Fig. 4. Integrated mass versus radius: total gravitational mass (solid line) and gas mass (dotted line). A typical error bar is shown at r_{500}. The total mass profile taking into account a temperature gradient (dashed line) is shown up to the radius to which the temperature gradient can be determined.

interaction between the radio lobes and the intra-cluster gas will be studied in detail.

Acknowledgements. We thank D. Burke and V. Hambaryan for help with the data analysis and P. James for carefully reading the manuscript.

References

Cavaliere, A., & Fusco-Femiano, R. 1976, A&A, 49, 137
Churazov, E., Brüggen, M., Kaiser, C. R., Böhringer, H., & Forman, W. 2000 [astro-ph/0008215]
Condon, J. J., Cotton, W. D., Greisen, E. W., et al. 1998, AJ, 115, 1693
David, L. P., Nulsen, P. E. J., McNamara, B. R., et al. 2000 [astro-ph/0010224]
Dickey, J. M., & Lockman, F. J. 1990, ARA&A, 28, 215
Ettori, S., & Fabian, A. C. 1999, MNRAS, 305, 834
Fabian, A. C. 2001, Proc. of the XXI Moriond Conf.: Galaxy Clusters and the High Redshift Universe Observed in X-rays, ed. D. M. Neumann, in press
Fabian, A. C., Sanders, J. S., Ettori, S., et al. 2000, MNRAS, 318, L65
Fischer, J., Hasinger, G., Schwope, A. D., et al. 1998, Astronomische Nachrichten, 319, 347
Heinz, S., Reynolds, C. S., & Begelman, M. C. 1998, ApJ, 501, 126
Huang, Z., & Sarazin, C. L. 1998, ApJ, 496, 728
Kaastra, J. S., & Mewe, R. 1993, A&AS, 97, 443
Liedahl, D. A., Osterheld, A. L., & Goldstein, W. H. 1995, ApJ, 438, L115
McNamara, B. R. 2001, Proc. of the IAP 2000 Conf. Constructing the Universe with Clusters of Galaxies, ed. F. Durret, & D. Gerbal [astro-ph/0012331]
McNamara, B. R., Wise, M., Nulsen, P. E. J., et al. 2000, ApJ, 534, L135
Mohr, J. J., Mathiesen, B., & Evrard, A. E. 1999, ApJ, 517, 627
Reynolds, C. S., Heinz, S., & Begelman, M. C. 2001, ApJ, 549, L179
Sarazin, C. L. 2001, Proc. of the XXI Moriond Conf: Galaxy Clusters and the High Redshift Universe Observed in X-rays, ed. D. M. Neumann, in press
Schindler, S. 1996, MNRAS, 280, 309
Schindler, S. 1999, A&A, 349, 435
Schwope, A., Hasinger, G., Lehmann, I., et al. W. 2000, Astronomische Nachrichten, 321, 1